Charge motion in MbCO crystals after flash photolysis

Icko E. T. Iben, Lajos Keszthelyi,* Dagmar Ringe,‡ and György Váró*
Department of Physics, University of Illinois at Urbana-Champaign, Urbana, Illinois 61801; *Institute of Biophysics, Biological Research Center, Hungarian Academy of Sciences, Szeged, Hungary; and ‡Department of Chemistry, Massachusetts Institute of Technology, Cambridge, Massachusetts 02139

ABSTRACT Charge motion accompanying the dissociation and recombination of carbon monoxide to oriented myoglobin crystals has been observed. The magnitude of the electrical signals detected after photodissociation by electrodes on either side of MbCO crystals of type A is consistent with the x-ray data showing that the doubly charged iron ion lies in the mean heme plane when a ligand is bound and moves out of the plane when deligated. Beyond 10 ms, the time development of the electrical signal is consistent with the kinetics observed optically after flash photolysis on the same crystals.

INTRODUCTION

The activity of many enzymes and proteins is accompanied by charge motion. In heme proteins such as ferrous (Fe^{+2}) myoglobin (Mb), the charge motion is easily described. The active center of Mb is formed by a heme group with a central iron ion (Fe). The Fe ion has six coordination sites. Four sites are covalently bound to nitrogens of the porphyrin. The fifth site is bound to the distal histidine, residue F7. To the sixth site of the Fe ion, ligands such as O_2 and CO can bind reversibly. In the ferrous state, the Fe ion is nominally doubly charged, +2e. Charge neutrality of the protein is maintained by the porphyrin ring which carries a charge of −2e. When carbon monoxide (CO) is bound to the Fe, it lies in the mean heme plane. Upon deligation, the Fe moves ~40 pm out of the mean heme plane (1–4) within 350 fs (5). When the proteins are oriented, a net polarization current results from the motion of the Fe ion during the process of ligation and deligation. By placing electrodes across oriented proteins, polarization currents can be detected (6, 7). Here we report the direct observation of electrical signals resulting from charge motion in oriented carbonmonoxy-myoglobin (MbCO) crystals.

We measure the voltage developed across MbCO crystals as a function of time after photodissociation, using the technique of protein electric response signals (PERS) (6). The PERS measurements demonstrate that a net polarization does accompany the dissociation and binding of CO to Mb^{+2} at pH ~6.5. Rebinding was also monitored optically. The optical measurements show that for times longer than 10 μs, rebinding in crystals at room temperature can be characterized by a bimolecular process with a single second-order rate coefficient on the order of $(7 \pm 3) \times 10^5\ M^{-1}s^{-1}$. The electrical measurements can be fit assuming that the PERS signal is due to the Fe^{+2} ion moving 40 pm out of and into the heme plane upon photolysis and recombination. A fraction 0.3 rebinds geminately with a time constant of 3 ± 1, μs, whereas the remaining 0.7 rebind with the same bimolecular process as seen in the optical measurements.

Dr. Iben's present address is AT&T Bell Laboratories, 1A-135, 600 Mountain Avenue, Murray Hill, NJ 07974.

EXPERIMENTAL PROCEDURE

The MbCO crystals were of the monoclinic form (type A) and are in the P_{21} space group. The dimensions of a unit cell are: (a, b, c) = (6.43, 3.09, 3.49 nm), with orientation (α,β,γ) = (90, 105.85, 90°), and c^* = 0.02983 (8). Viewed macroscopically, the crystals are flattened four-sided prisms. The b-axis is along the long axis of the crystal, the a-axis is the width, and the c-axis essentially the depth of the crystal. Within each unit cell there are two protein molecules. The two hemes are related to one another by a 180° rotation about the b-axis followed by a translation of one half the unit cell length, b (1.54 nm) (Fig. 1). The plane of each heme is essentially perpendicular to the a-b plane, with angles of +112° and −112°, respectively, to the b-axis.

The crystals were kept in a mother liquor of 75% saturated ammonium sulfate buffered with 0.1 M potassium phosphate to pH ~6.5. The reduction of the crystals proceeded as follows. (a) Place the crystals and mother liquor in a gas exchange bulb, exchange the gas above the crystals with N_2 gas, and allow the gas to mix for 24 h. (b) Add dithionite to make a 10 mM concentration, and allow 24 h for mixing. (c) Add more dithionite to make a 20 mM solution, and allow another 24 h for mixing. (d) Exchange the N_2 gas above the crystals with CO at normal atmospheric pressures, allow 1 wk for complete mixing, daily exchanging the gas with fresh CO to avoid O_2 contamination.

The photolyzing rhodamine dye laser, 590 nm, with an energy of ~10 mJ and pulse width of ~1 μs (FWHM), was focused to about the size of a single crystal. The crystal was placed on a glass shelf of the rotating stage of an optical microscope. A drop of mother liquor covered the crystal, and another glass side was suspended over the drop. This arrangement served both to seal CO gas in the solution and to prevent

0006-3495/89/09/459/05 $2.00

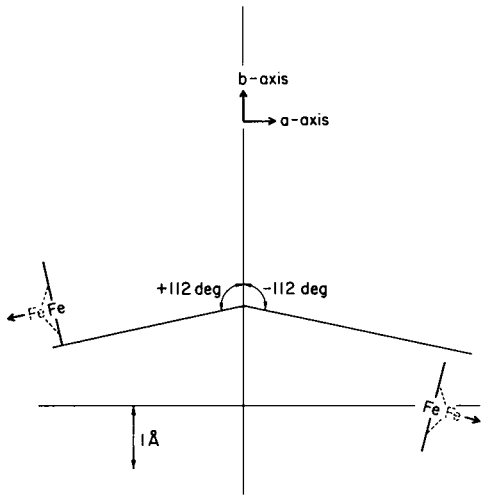

FIGURE 1 Schematic of Mb crystals, type A. The arrows emanating from the iron, Fe^{+2}, show the direction they move after delegation of the CO. Solid lines passing through the Fe^{+2} represent the heme; dashed lines represent the heme buckling.

refraction of the monitoring light by the meniscus of the solution. The alignment of the crystal was checked by viewing through the microscope. For the electrical measurements, platinum electrodes were placed on opposite sides of the crystal and extended into the solution of conductivity ~150 mmho/cm (9). The ground electrode was soldered to the brass case that surrounded the crystal. Aluminum foil was placed below the glass rotating stage for electrical shielding, and a hole was cut to allow the photolyzing laser to pass. A small window in the top of the grounding shield allowed optical viewing of the orientation of the crystal and the electrodes. The signals from the electrodes were amplified by a homemade amplifier with a bandwidth of ~100 MHz at unity gain, built using a model 3554 op-amp (Burr-Brown Corp., Tucson, AZ). For the optical measurements a 632.8-nm helium-neon laser was used to monitor the changes in absorption as a function of time after photodissociation. To avoid stray light, the crystal was masked with the iris of the microscope. The optical signal was detected with a photodiode. The system trigger was a photodiode activated by light from the photolyzing laser. All signals were stored in a transient recorder with linear time base (product of the Central Research Institute of Physics, Budapest, Hungary).

MODEL

In the analysis we assume that the signals originate from charge motions related to CO release and rebinding. We will elaborate on this assumption in Results and Discussion. To analyze the electrical signals, we modeled the electrical system with an equivalent circuit of resistors and capacitors (6) as shown in Fig. 2. The elements should be compared with the actual physical setup (Fig. 3). R_e is the effective resistance between the crystal and the platinum electrode. The capacitance between the crystal and the electrodes does not change the analysis

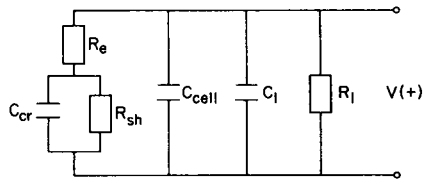

FIGURE 2 Equivalent circuit for analyzing the charge motion in the photodissociated MbCO crystals. Elements are labeled as described in Model section.

and has been left out for simplicity. C_{cr} and R_{sh} are of the same order of magnitude and are determined by the resistance of the solution, which is estimated to be of the order of 1 kohm. C_d is the effective capacitance of the cell and the measuring electronics ($C_{cell} + C_i$) and is of the order of 20 pF. R_i is the amplifier resistance to ground, which was 1 kohm.

If the polarization of the molecules within the crystal changes, then a bound surface charge, Q_b will develop across the crystal. Assuming spherical geometry for the crystal in a medium of dielectric strength ϵ:

$$Qb(t) = -[(pN_oA)\left(\frac{3}{2\epsilon + 1}\right)\cos\theta]N(t). \quad (1)$$

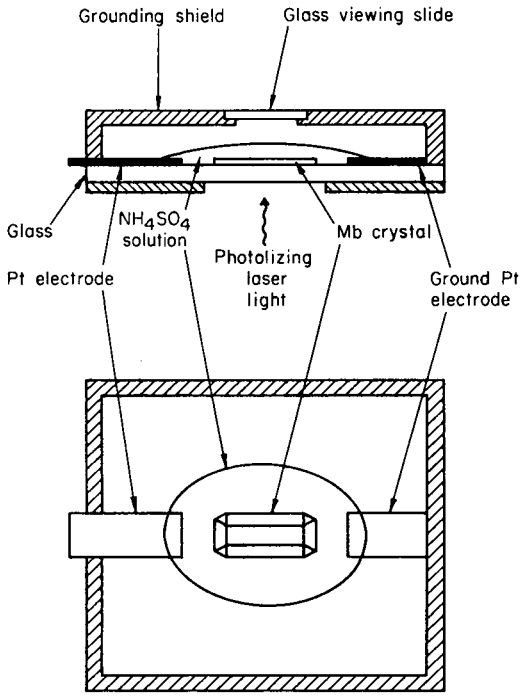

FIGURE 3 Schematic of the setup for mounting the crystals and measuring the electric PERS signal.

Here $N(t)$ is the fraction of unbound proteins as a function of time, t, after the laser flash; p is the change in dipole moment per protein caused by dissociation; θ is the angle between $\vec{p}$ and the b-axis. N_0 is the protein concentration; A is the area of the illuminated portion of the crystal; ϵ is the dielectric coefficient of the solution. The bound surface charge will in turn charge up C_d, which discharges through the parallel resistance of R_l with $(R_e + R_{sh})$, termed R_d. The time dependence of this voltage, $V_c(t)$, is calculated using Eq. 1 and Kirchoff's laws for the effective circuit, Fig. 3.

$$V_c(t) = V_0 \int_0^t dt_1 \frac{dN(t_1)}{dt_1} \{\exp[-(t - t_1)/\tau_d] - \exp[-(t - t_1)/\tau_c]\} \quad (2a)$$

$$V_0 = [Q_b(0)/C_d]R_{sh}/R_d. \quad (2b)$$

With a filter time constant, τ_f, the measured voltage is

$$V(t) = \int_0^t \frac{dt_2}{\tau_f} V_c(t_2)\, e^{-(t-t_2)/\tau_f}. \quad (2c)$$

Here, τ_c $[\sim C_{cr}R_eR_{sh}/R_d]$ is the charging time of C_d. Because τ_c is of the order of 10 ps, it is ignored in our analysis. $\tau_d \sim R_dC_d$ is the discharge time of C_d and is estimated to be ~20 ns. The factor, R_{sh}/R_d is the fraction of charge that accumulates on C_d before discharging, rather than merely discharging directly across R_e. $dN(t)/dt$ is the rate of change of the number of unbound proteins, $N(t)$, as a function of time. Because the time for delegation is so short (350 fs), the rise of $N(t)$ is determined by the flashoff rate, K_0 whereas the decay of N(t) is governed by the subsequent recombination kinetics.

RESULTS AND DISCUSSION

Fig. 4, *a*, *d*, and *e*, shows electrical signals resulting from photolysis of MbCO at pH 6.5 by 2-μs laser pulse when the *b*-axis of the crystal was aligned along the line connecting the two electrodes (zero-degree orientation). The electric field polarization of the laser, $\vec{E}_{ias}$, was aligned along the crystal *b*-axis. To be certain that the signals obtained were due to charge motion accompanying photodissociation and recombination, we performed several tests. In the absence of a crystal, the laser was swept horizontally across the sample cell from one electrode to the other. When the laser struck either electrode, a large electrical signal was registered, of opposite sign for each electrode. By focusing the photolysing laser beam between the electrodes this effect was minimized, while subtraction of signals taken by rotating the electrodes 180° about the optical axis left only electrical noise. With an MbCO crystal centered between the electrodes and the laser focused on the crystal, ($\vec{E}_{ias}$ aligned along the *b*-axis), we obtained the data seen in Fig. 4 *d*. Rotation of the crystal by 180° about the c^* axis resulted in a signal of the same magnitude but opposite polarity (Fig. 4 *a*). Rotation of the crystal by 90° about the same axis ($\vec{E}_{ias}$ aligned along the *a*-axis) left only electrical noise (Fig. 4 *b*).

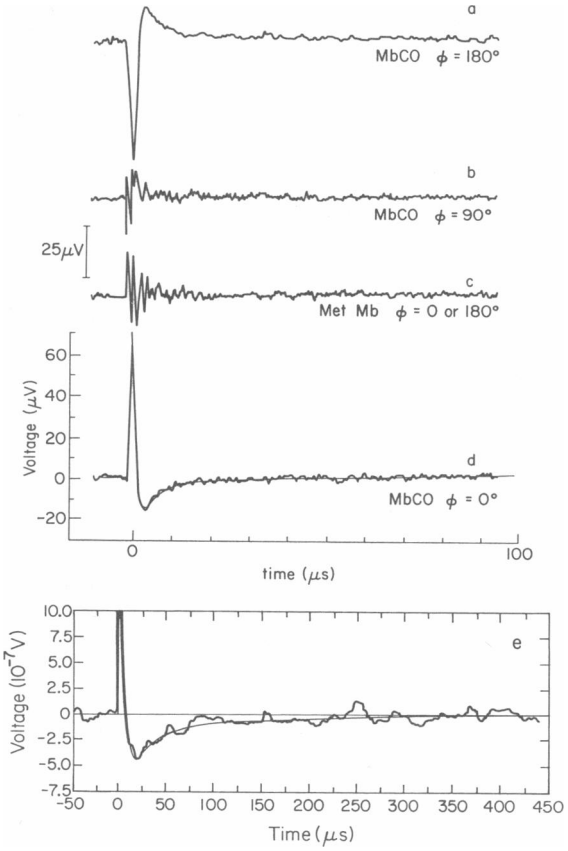

FIGURE 4 Electric signals resulting from photolyzed type A Mb crystals using the setup in Fig. 2. All voltages are normalized to a single shot with unity gain. The smooth lines through the data of *d* and *e* are fits using the model and parameters given in the analysis section. (*a*) MbCO: 180° orientation (25 shots, gain = 10^3, τ_f = 1 μs). The fit is described in Results and Discussion. (*b*) MbCO: 90° orientation (25 shots, gain = 10^3, τ_f = 1 μs). (*c*) metMb: 0° orientation (25 shots, gain = 10^3, τ_f = 1 μs). (*d*) MbCO: 0° orientation (25 shots, gain = 10^3, τ_f = 1 μs). (*e*) MbCO: 0° orientation (25 shots, gain = 10^4, τ_f = 5 μs). The fit is described in the Results and Discussion.

Note that the absence of a clear PERS signal for the 90° orientation is not due to the lack of photolysis. Assuming that the protein absorption dipole moment is in the heme plane, the extinction coefficient for E_{ias} polarized along the *b*-axis would be only 2.5 times that for E_{ias} polarized along the *a*-axis (cos[22°]/sin[22°] ~ 2.5). In actuality, with the large extinction coefficient for light

polarized along the b-axis (>2 OD for 0.1 mm) the decrease in extinction coefficient for light polarized along the a-axis (Fig. 1) would result in an increase in flashoff (~50% greater).

The absorption of 10 mJ of energy by such an optically concentrated sample surely results in some heating. To rule out piezoelectric or pyroelectric effects, a control was performed using met Mb crystals, Fe^{+3}. With the crystal b-axis and $\vec{E}_{ias}$ aligned along the electrodes only the electrical ringing similar to that seen for MbCO at a 90° orientation was registered, (Fig. 4 c). Thus, the PERS signals shown in Fig. 4, a, d, and e, are a result of delegation and subsequent ligation of Mb with CO rather than piezoelectric or pyroelectric effects.

The positive voltage spike seen in Fig. 4 d is assigned to the iron moving out of the main heme plane after photodissociation. Using Eq. 1 with $A = 5. \times 10^{-3}$ cm^2, p = 3.8 debye ($p_{Fe} \sim 2\ e \times 40$ pm), $\theta = 112°$, $\epsilon = 80$, and $N(t_l) = 0.29$ (integrating Eq. 4 across the thickness of the crystal $L \sim 0.1$ mm, with $N_\nu \sim 7$) a value of $Q_b \sim 0.4 \times 10^{-12}$ coul is obtained.

Using Eq. 2, a–c, with $dN(t)/dt = k_0 e^{-k_0 t}$ during photolysis ($t \leq \tau_l$), the peak voltage due to the Fe^{+2} ion moving out of the heme plane is

$$V(\tau_l) \sim V_0 \left(\frac{k_0 \tau_d}{1 - k_0 \tau_f}\right)(e^{-\tau_l/\tau_f} - e^{-k_0 \tau_l}), \qquad (3)$$

with $k_0 \sim 3 \times 10^6$ s^{-1}, (0.3 μs saturation time, $\tau_f \sim 1$ μs, and the other parameters as given earlier, $V(\tau_l = 1.5\ \mu s) = 67\ \mu V$, as compared to the 60 ± 5 μV of Fig.4, a and b. The fit is shown in Fig. 4 d. When ligands recombine, the ion will move back into the heme plane, resulting in a current of opposite sign to that of the out-of-plane motion. Fig. 4, a and b, clearly shows a current of opposite sign to the out-of-plane motion with a time course of ~3 μs. Fig. 4 e shows the longer time PERS signal, registering beyond 50 μs.

As a companion, recombination was monitored optically as a function of laser intensity. Due to the close proximity of the photolysis, 590 nm, and the monitoring, 632.8 nm, only laser beam data beyond 10 μs could be measured. Assuming two states for each protein, ligated vs. unligated, the change in absorbance, $\Delta A(t)$, is proportional to the number of unbound ligands, $n(t)$. In this paper, $\Delta A(t)$ was fit with a bimolecular reaction model. Assuming the product of the second order rate coefficient, k_{bm}, the CO concentration in the solution, $[CO]_o$ (~1 mM [10]) multiplied by the time after photolysis t, is small ($k_{bm}[CO]_o 4.0 \times 10^{-4}$ s ~ 0.3), the exact bimolecular reaction reduces to a power law:

$$N(t)_{bm} \sim N_o \int_0^L \frac{dx}{L} \frac{f(x)}{(1 + f(x) k_{bm} N_o t)}, \qquad (4)$$

where $N(t)_{bm}$ is the number of unligated proteins, N_o is the protein concentration (~48 mM; reference 8), k_{bm} is the second order rate coefficient; $f(x)$ is the fraction of proteins photodissociated as a function of depth into the crystal; L is the thickness of the crystal. Because the optical absorption is so large at the photolyzing wavelength, $N_o\sigma \sim 200$ cm^{-1}, (σ is the extinction coefficient at the photolyzing wavelength of 590 nm), $f(x)$ is a strong function of depth into the crystal. Using Poisson statistics, $f(x)$ is given as

$$f(x) = [1.0 - \exp(-N_\nu\ 10^{-N_o \sigma x}). \qquad (5)$$

N_ν is the number of photons absorbed per protein at the surface of the crystal and was around seven in these experiments. The optical data (Fig. 5) is fit with a bimolecular process having a second order rate of $k_{bm} = (7 \pm 3) \times 10^5$ M^{-1} s^{-1} (11). The electrical signals can be fit if a geminate process is included, where 30% of the photodissociated proteins recombine exponentially with a 3 μs time constant. The remaining 70% recombine via the bimolecular process used to fit the optical data (Fig. 4, d and e).

CONCLUSION

The magnitude and time response of the electrical signal that occurs during the laser pulse is consistent with the Fe^{+2} ion moving ~40 pm out of the heme plane within 350 ps of photolysis. Another possible contribution to the PERS signals is the CO dipole moment, $p_{co} = 0.112$ debye (9). Because $p_{co}/p_{Fe} \sim 0.03$, the contribution of p_{co} to the PERS signals is ignored. As for other sources of large motion, these cannot be ruled out due to the uncertainty in the parameters such as R_{sh}, R_e, τ_d, and c_d used to make the calculations. The long term PERS signals do follow

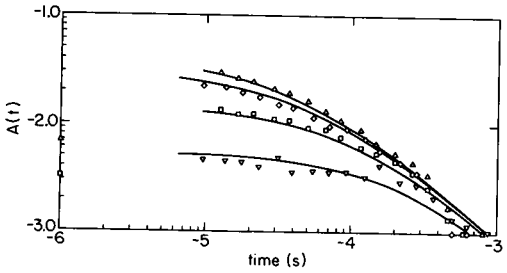

FIGURE 5 Rebinding curves as a function of photolyzing laser intensity for type A MbCO crystals, monitored with a He-Ne laser at 632.8 nm. The four curves represent kinetics resulting from photolyzation at various fractions of full intensity (10 μJ) of the photolyzing laser: Δ full intensity, ◊ 0.50 OD filter, □ 1 OD filter, ▽ 1.5 OD filter. In all cases, a second, long-lived process (>10 ms), which accounted for 10% of the signal amplitude, was subtracted off. Lines through the data are fits using the model and parameters described in Results and Discussion.

the time course of the recombination as measured in the optical data, accounting for ~70% of the charge measured in the out of plane motion. The additional 3 μs relaxation having charge motion opposite to the out of plane signals and accounting for 30% of the charge can be explained by a geminate recombination process. Studies of CO recombination to Mb in viscous mediums such as dried polyvinyl-alcohol (PVA) (12), 99% glycerol-water (13), and MbCO under pressures of 1–2 MPa (Frauenfelder, H., University of Illinois at Urbana-Champaign, unpublished data) show a marked increase in a fast geminate process. The most viscous of these mediums at room temperature, PVA, results in ~30% of the MbCO's recombining within 10 μs via a geminate process. Thus, a fraction of 30% geminate process is possible for recombination in crystalline MbCO. This does not rule out additional charge motions within the protein of the order of 1 debye as a source of the 3 μs process.

Though the extraction of accurate physical parameters from the data is a difficult task, several steps might improve the situation. Firstly, the magnitude of the signals can be greatly enhanced if the shunt resistance, R_{sh}, is increased. In our case, we had a dissipation time of ~20 ns, whereas the charge motion occurred with rates from 1 μs to 10 ms. In this case, the short dissipation times decreased the signal amplitudes by two to six orders of magnitude. In some instances, such as membrane proteins, R_{sh} is naturally much larger (6). Many biological substances, though, form crystals only in highly conductive salt solutions, but once they are formed they can be washed clean and transferred to a less conductive solvent.

Another difficulty in these experiments is that the internal resistances are unknown. Consequently, the extraction of the dipole moment, p, remains uncertain. By choosing a laser pulse time that is much faster than τ_d, the value of τ_d can be measured kinetically as the decay of the charge-buildup signal. Furthermore, by varying C_l and R_l, one can hope to make accurate measurements of C_d and τ_d, and therefore also of p. A direct consequence of the necessity of using oriented samples for PERS measurements is that the absorption of polarized light by the samples is strongly dependent on orientation. To obtain quantitative results, it is necessary to use polarized light and to know the angular dependence of the cross-section. For Mb crystals, type A, the ratio of cross-sections at 590 nm, along the a- and b-axes, is at least 15:1 (14). By rotating the photolyzing laser polarization from the b- to the a-axis, the magnitude of the fraction of proteins flashed off is changed dramatically. For bimolecular reactions, this can change the recombination times significantly. Furthermore, if the monitoring beam is unpolarized, then the optical signals can be greatly distorted from simple Beer's law absorption. Therefore, great care must be taken to measure and record the orientations of the crystal, the photolyzing light, and the monitoring light.

We thank A. Ansari, B. Cowen, H. Frauenfelder, P. Ormos, T. Sauke, and E. Shyamsunder for helpful discussions and critical comments, and Mary Ostendorf for typing the manuscript.

This work was supported in part by United States Public Health Service grant GM18051 from the Department of Health and Human Services, by the Madgyar Tudomanos Academiz, Szeged, Hungary, by the Joint American National Science Foundation/Hungarian Academy of Science, National Science Foundation grant NINT82-17661, and by the Physics Department of the University of Illinois, Urbana, IL.

Received for publication 7 December 1988 and in final form 19 May 1989.

REFERENCES

1. Takano, T. 1977. Structure of myoglobin refined at 2.02 Å resolution II. Structure of deoxymyoglobin from sperm whale. *J. Mol. Biol.* 110:569–584.
2. Phillips, S. E. V. 1980. Structure and refinement of oxymyoglobin at 1.6 Å resolution. *J. Mol. Biol.* 142:531–554.
3. Phillips, S. E. V. 1978. Structure of myoglobin. *Nature (Lond.).* 273:247–248.
4. Norvell, J. C., A. C. Nunes, and B. P. Schoenborn. 1975. Neutron diffraction analysis of myoglobin: structure of the carbon monoxide derivative. *Science (Wash. DC).* 190:568–570.
5. Martin, J. L., A. Mihgus, C. Poyart, Y. Lecarpentier, R. Astier, and A. Antonetti. 1983. Femtosecond photolysis of CO-liganded protoheme and hemoproteins: appearance of deoxy species with a 350-free time constant. *Proc. Natl. Acad. Sci. USA.* 80:173–177.
6. Keszthelyi, L. and P. Ormos. 1983. Displacement current on purple membrane fragments oriented in a suspension. *Biophys. Chem.* 18:397–405.
7. Lindau, M., and H. Rüppel. 1983. Evidence for conformational substaters of rhodopsin from kinetics of light-induced charge displacement. *Photobiochem. Biophys.* 5:219–228.
8. Kendrew, J. C. and R. G. Parrish. 1956. The crystal structure of myoglobin. III. Sperm-whale myoglobin. *Proc. R. Soc. A.* 238:305–324.
9. Weast, R. C., editor. 1975. Handbook of Chemistry and Physics. 56th ed. CRC Press, Inc., Boca Raton, FL.
10. Wilhelm, E., R. Batino, and R. J. Wilcock. 1977. Low-pressure solubility of gases in liquid water. *Chem. Rev.* 77:219–262.
11. Antonini, E., and M. Brunori. 1971. Hemoglobin and Myoglobin in Their Reaction with Ligands. North-Holland Publishing Co., Amsterdam.
12. Austin, R. H., K. W. Beeson, L. Eisenstein, H. Frauenfelder, and I. C. Gunsalus. 1975. Dynamics of ligand binding to myoglobin. *Biochemistry.* 14:5355.
13. Beece, D., L. Eisenstein, H. Frauenfelder, D. Good, M. C. Marden, L. Reinisch, A. H. Reynolds, and L. B. Sorensen. 1980. Solvent viscosity and protein dynamics. *Biochemistry.* 19:5147–5157.
14. Lever, A. B. P. and H. B. Gran, editors. 1982. Iron Prophyrins. Part I. Addison-Wesley Publishing Co., Reading, MA.